Alexandria Engineering Journal (2022) 61, 9175–9186

HOSTED BY

Alexandria University

Alexandria Engineering Journal

www.elsevier.com/locate/aej
www.sciencedirect.com

On a new and generalized fractional model for a real cholera outbreak

Dumitru Baleanu [a,b,c], **Fahimeh Akhavan Ghassabzade** [d], **Juan J. Nieto** [e], **Amin Jajarmi** [f,*]

[a] *Department of Mathematics, Faculty of Arts and Sciences, Çankaya University, 06530 Ankara, Turkey*
[b] *Institute of Space Sciences, P.O. Box, MG-23, R 76900 Magurele-Bucharest, Romania*
[c] *Department of Medical Research, China Medical University Hospital, China Medical University, Taichung, Taiwan*
[d] *Department of Mathematics, Faculty of Sciences, University of Gonabad, Gonabad, Iran*
[e] *Instituto de Matemáticas, Universidade de Santiago de Compostela, 15782 Santiago de Compostela, Spain*
[f] *Department of Electrical Engineering, University of Bojnord, P.O. Box, 94531-1339 Bojnord, Iran*

Received 28 November 2021; revised 12 February 2022; accepted 21 February 2022
Available online 28 February 2022

KEYWORDS

Fractional derivative;
General kernel;
Cholera outbreak;
Stability analysis;
Numerical method;
Product-integration rule

Abstract In this paper, a new mathematical model involving the general form of Caputo fractional derivative is studied for a real case of cholera outbreak. Fundamental properties of the new model including the equilibrium points as well as the basic reproduction number are explored. Also, an efficient approximation scheme on the basis of product-integration rule is established to solve the new model. Several kernel functions for the general fractional derivative are tested, and the results are compared with the real data of a cholera outbreak in Yemen. As a consequence, we find a special case in which the aforesaid outbreak is described better, for the corresponding numerical simulations are closer to the real data than the other classical and fractional frameworks. Next, we apply the most realistic model to investigate the effect of vaccination on the considered cholera outbreak. Simulation results show that earlier vaccination could reduce the number of infected individuals effectively, so mortality would have been reduced considerably if the vaccination had been performed earlier.

1. Introduction

Cholera is a subject that concerns all human races. This infectious illness prompts severe watery diarrhea. Diarrhea can be such drastic that it leads within hours to intensive dehydration and electrolyte unbalance. This may result in bruised and cold skin, wrinkled hands and feet, sunken eyes, and diminished skin elasticity. Symptoms begin two hours to five days after the exposure. This illness is caused by eating unsafe food and drinking unsafe water infected with a bacterium named

* Corresponding author.
E-mail address: a.jajarmi@ub.ac.ir (A. Jajarmi).

Peer review under responsibility of Faculty of Engineering, Alexandria University.

https://doi.org/10.1016/j.aej.2022.02.054

Vibrio cholera [1]. This disease had been widespread in the US before that the modern water and sewage treatment systems omitted their spread via contaminated water [2]. Researchers have estimated that every year, there are roughly 1.3 to 4.0 million cholera cases in endemic countries, and 21000 to 143000 deaths occur worldwide due to this disease [3]. In 2010, cholera was classified as a pandemic illness. Southeast Asia and Africa are the areas with an ongoing risk of spreading the disease. The risk of death amongst infectious persons is usually fewer than five percent, but it may increase to fifty percent. Lack of treatment facilities leads to higher death rates [4]. The largest outbreak of cholera in the history happened in Yemen [5].

Mathematical models can help public health interventions by showing the likely outcome of an epidemic [6]. Also, these models can project how infectious diseases progress [7]. Researchers in the field of mathematical modelling examined several models for epidemic outbreaks. For instance, the authors in [8] explored a stochastic norovirus epidemic model with a time delay and random perturbations. In [9], a mathematical model for cholera considering the vaccination effects was proposed. In [10], Capasso and Paveri-Fontana suggested a mathematical model for the 1973 cholera epidemic in the European Mediterranean region. In 2017, the transmission dynamic of cholera in Yemen was investigated by Nishiura et al. [11]. A model containing optimal intervention strategies for cholera control was formulated in [12], a study which presented the optimal quarantine approach for the minimization of the number of infectious people. In this direction, another relevant research can also be found in [13].

Mathematical models based on integer-order differential equations explain the interactions between different parts of a realistic system under consideration, but it is a traditional approach in the concept of modelling [14]. Recently, there has been much interest in developing mathematical models by fractional-order differential equations (FDEs) [15]. The FDEs are naturally related to the systems with memory that exists in various real-world systems [16]. Over the past few years, the theory and application of FDEs have widely been explored by many researchers. In [17], a fractional description of a prey-predator model was studied, and its existence theory and numerical analysis were also investigated. In [18], the authors formulated a fractional tuberculosis model and evaluated the values of parameters according to the real clinical cases of tuberculosis infections in Yemen from 2000 to 2019. In [19], a local fractional Yang-Laplace decomposition method was extended to solve a nonlinear system of local fractional partial differential equations. In [20], a generalization of truncated M-fractional derivative was investigated, and its applications to FDEs were analyzed. In [21], the authors established some useful integral formulas by using fractional operators with generalized (p,q)-Mathieu type series. In 2020, Evirgen et al. [22] developed a comprehensive fractional analysis for an HIV infection model of $CD4^{+}T$ cells. In [23], a fractional model was considered for COVID-19 pandemic by taking into account the fear effects of the media and social networks. For the spread of COVID-19, a fractional model was also explored in [24] based on nonlocal differential operators. Another relevant study in the field of fractional calculus was performed in [25] in which the authors introduced a fractional model for the simulation of Ebola outbreak. In [26], a nonstandard finite difference scheme was employed for the modelling and synchronization of fractional chaotic systems.

In 2016, Luchko and Yamamoto [27] suggested a novel differential operator with a general kernel function. This degree-of-freedom provides a broad range of applications due to the existence of flexibility in choosing the kernel [28]. By changing the kernel in the general derivative, various asymptotic behaviours are obtained. This fact helps to show the hidden features of real-world systems more accurately than the traditional fractional systems. Nonetheless, the properties and applications of this new operator must be explored more in practical situations, and some complete theorems must also be developed to analyze this operator. Besides, some appropriate analytical and numerical methods should be investigated to solve the fractional equations including the aforesaid general operator. Motivated by the above discussion, this research suggests a novel mathematical model involving the general form of Caputo fractional derivative for a real case of cholera outbreak. The novelty of this research comes from the fact that, to the best of our knowledge, no previous study has analyzed a mathematical model with the general form of fractional derivative for the cholera disease, an advantage which increases the degree-of-freedom by using different kernels and various fractional orders in order to capture the hidden aspects of biological system under investigation. The main contributions of this research and the new achievements obtained within this manuscript are summarized as follows:

- This paper addresses a new mathematical model of cholera disease, which involves the general form of Caputo fractional derivative.
- The fundamental characteristics of the new model are discussed in detail.
- To solve the suggested model, an effective approximation technique on the basis of product-integration rule is developed.
- Several specific cases of general kernel are considered, and the effect of vaccination on the spread of cholera is also investigated by means of the new model.
- Comparative results in this reseach show an obvious linkage between the mathematical and biological mechanisms.

Consequently, we think the work carried out in this study makes the research rich in the new direction of fractional calculus and presents promising results for the analysis, control, and prevention of cholera outbreak.

The rest of this paper is structured in the following way. The elementary concepts of general fractional derivative are given in Section 2. Section 3 focuses on the new fractional model. In Section 4, the basic properties of the new model are discussed. For the purpose of implementation, an efficient numerical method is proposed in Section 5, and the analysis of numerical results is also included in this section. Eventually, a sum up for the paper is given in Section 6.

2. Preliminary remarks

In this section, we present a brief review of notations and preliminaries for fractional derivatives and integrals in a new general form.

Definition 2.1 [27]. The left-sided fractional derivative of Riemann-Liouville type in general sense is defined by

$$ {}_0\mathscr{D}_t^q f(t) = \frac{d}{dt}\int_0^t f(x)\kappa_L(t-x)dx, \tag{1} $$

and the general form of Caputo derivative is described as

$$ {}_0^C\mathscr{D}_t^q f(t) = \int_0^t f'(x)\kappa_L(t-x)dx, \tag{2} $$

where $0 < q < 1$ demonstrates the fractional-order, $f:[0,+\infty)\longrightarrow\mathbb{R}$ is an absolutely continuous function satisfying $f' \in L^1_{loc}(0,+\infty), 0 \leqslant t \leqslant T < +\infty$, and the general kernel κ_L is a locally integrable nonnegative function. The relation between the Riemann-Liouville and Caputo fractional derivatives (1) and (2) is also stated as [27]

$$ {}_0\mathscr{D}_t^q f(t) = {}_0^C\mathscr{D}_t^q f(t) + \kappa_L(t) f(0). \tag{3} $$

Remark 2.1. The operators (1) and (2) are linear, so

$$ {}_0\mathscr{D}_t^q(c_1 f_1(t) + c_2 f_2(t)) = c_1\,{}_0\mathscr{D}_t^q f_1(t) + c_2\,{}_0\mathscr{D}_t^q f_2(t), \tag{4} $$

$$ {}_0^C\mathscr{D}_t^q(c_1 f_1(t) + c_2 f_2(t)) = c_1\,{}_0^C\mathscr{D}_t^q f_1(t) + c_2\,{}_0^C\mathscr{D}_t^q f_2(t). \tag{5} $$

Similarly, the right-sided general fractional derivatives are described by [27]

$$ {}_t\mathscr{D}_T^q f(t) = \frac{d}{dt}\int_t^T f(x)\kappa_R(x-t)dx, \tag{6} $$

$$ {}_t{}^C\mathscr{D}_T^q f(t) = \int_t^T f'(x)\kappa_R(x-t)dx, \tag{7} $$

where κ_R has the same properties as κ_L.

The above introduced general operators agree with the generalization in [29]. Thus, according to the analysis in [29], the aforesaid operators satisfy the integration-by-parts formulas in the following way

$$ \int_0^T f(x)\,{}_0\mathscr{D}_x^q g(x)dx = \int_0^T g(x)\,{}_x{}^C\mathscr{D}_T^q f(x)dx, \tag{8} $$

$$ \int_0^T f(x)\,{}_0^C\mathscr{D}_x^q g(x)dx = \int_0^T g(x)\,{}_x\mathscr{D}_T^q f(x)dx. \tag{9} $$

Remark 2.2. There exists a completely monotone function $m_L(t)$ so as under some suitable conditions on the kernel function $\kappa_L(t)$, the convolution $\kappa_L(t) * m_L(t)$ is equal to 1 [27], *i.e.*,

$$ \kappa_L(t) * m_L(t) = \int_0^\infty \kappa_L(t-x)m_L(x)dx = 1,\ t > 0. \tag{10} $$

Lemma 2.1 [27]. *Suppose that $f \in L_1^{loc}(\mathbb{R}^+)$; then we have*

$$ {}_0\mathscr{I}_t^q\left[{}_0^C\mathscr{D}_t^q f(t)\right] = f(t) - f(0), \tag{11} $$

where ${}_0\mathscr{I}_t^q$ indicates the Riemann-Liouville fractional integral in general sense portrayed via

$$ {}_\mathscr{I}{}_t^q f(t) = \int_0^t f(x)m_L(t-x)dx. \tag{12} $$

There are some specific cases in agreement with the above-expressed definitions:

- If we set $\kappa_L(t) = \frac{t^{-q}}{\Gamma(1-q)}$, then m_L becomes the power function $\frac{t^{q-1}}{\Gamma(q)}$. In this case, the general operators (1) and (2) are demoted to the classical Riemann-Liouville and Caputo fractional derivatives, respectively. Moreover, the integral operator (12) is reduced to the Riemann-Liouville integral [30].
- If we set $\kappa_L(t) = \frac{\chi(q)}{1-q}E_q\left[\frac{-q}{1-q}t^q\right]$, where E_q is a Mittag-Leffler (ML) function and $\chi(q)$ is a normalization function fulfilling $\chi(0) = \chi(1) = 1$, then we obtain the nonlocal and nonsingular AB-Caputo derivative operator [31].
- If we set $\kappa_L(t) = \frac{\chi(q)}{1-q}\exp\left[\frac{-q}{1-q}t\right]$, where $\chi(q)$ is a normalization function as above, then the Caputo-Fabrizio derivative operator is obtained [32].

3. New mathematical model

In [1], Lemos-Paião et al. suggested a conceptual model for the cholera disease, which effectively catched the time-line of a cholera outbreak. Indeed, the authors in [1] formulated the mathematical epidemic model of cholera including five components as

$$ \begin{cases} S'(t) = \Lambda - \mu S(t) + \varphi R(t) - \frac{\beta S(t)}{C(t)+\rho}C(t), \\ I'(t) = -(\alpha_1 + \mu + \gamma)I(t) + \frac{\beta S(t)}{C(t)+\rho}C(t), \\ Q'(t) = -(\alpha_2 + \mu + \epsilon)Q(t) + \gamma I(t), \\ R'(t) = -(\varphi + \mu)R(t) + \epsilon Q(t), \\ C'(t) = -\sigma C(t) + \theta I(t), \end{cases} \tag{13} $$

accompanying with the initial conditions

$$ \begin{aligned} &S(0) = S_0, \quad I(0) = I_0, \quad Q(0) = Q_0, \\ &R(0) = R_0, \quad C(0) = C_0, \end{aligned} \tag{14} $$

where $S_0, I_0, Q_0, R_0, C_0 \geqslant 0$. In this model, $N(t)$ as the total population at time $t \geqslant 0$ is partitioned into four categories. The first-class contains susceptible individuals $S(t)$, the second class includes $I(t)$ as the infectious persons with symptoms, the individuals in treatment through a quarantine are in the third class and denoted by $Q(t)$, and the recovered persons $R(t)$ are in the final class. Additionally, $C(t)$ represents the bacterial concentration at time t. The parameter $\Lambda > 0$ shows the rate of recruitment in the susceptible class, and μ denotes natural death rate. The coefficient $\beta > 0$ represents the absorbency of the bacteria via taint sources. The infectious people can adapt to stay in quarantine at a time frame subject to an appropriate medicine at the rate γ. The bacteria population

half-saturation constant and the rate of losing immunity in the recovered individuals are denoted by ρ and φ, respectively. The recovery rate of quarantined individuals is described by ϵ. The two parameters α_1 and α_2 denote the rates of disease-related death in the persons that are contaminated and in quarantine, respectively. Also, the parameter θ shows the rate of bacterial concentration increase, and σ indicates the bacterial concentration decrease rate.

In 2018 [9], the model (13) was modified by considering different kinds of cholera's treatment and adding a vaccination class $V(t)$ as follows

$$\begin{cases} S'(t) = \Lambda - (\psi+\mu)S(t) + \varphi_1 R(t) + \varphi_2 V(t) - \frac{\beta S(t)}{C(t)+\rho} C(t), \\ I'(t) = -(\alpha_1+\mu+\gamma)I(t) + \frac{\beta S(t)}{C(t)+\rho} C(t), \\ Q'(t) = -(\alpha_2+\mu+\epsilon)Q(t) + \gamma I(t), \\ R'(t) = -(\mu+\varphi_1)R(t) + \epsilon Q(t), \\ V'(t) = -(\varphi_2+\mu)V(t) + \psi S(t), \\ C'(t) = -\sigma C(t) + \theta I(t), \end{cases} \tag{15}$$

where $\psi \geqslant 0$ shows the rate of vaccination in susceptible persons. The rates of losing immunity in the recovered and vaccinated individuals are also denoted by φ_1 and φ_2, respectively.

The integer-order models (13) and (15) do not save memory effects on themselves. To study the effects of memory in the above-mentioned epidemic models, we modify the model (15) to a fractional-order one, so we employ the general form of Caputo fractional derivative instead of ordinary time-derivatives in (15). Besides, we modify the fractional operator via an auxiliary parameter $\lambda > 0$ to avoid dimensional mismatching [33]. As a result, the new model takes the following form

$$\begin{cases} \lambda^{q-1}\,{}_0^C\mathscr{D}_t^q S(t) = \Lambda - (\psi+\mu)S(t) + \varphi_1 R(t) + \varphi_2 V(t) - \frac{\beta S(t)}{C(t)+\rho} C(t), \\ \lambda^{q-1}\,{}_0^C\mathscr{D}_t^q I(t) = -(\alpha_1+\mu+\gamma)I(t) + \frac{\beta S(t)}{C(t)+\rho} C(t), \\ \lambda^{q-1}\,{}_0^C\mathscr{D}_t^q Q(t) = -(\alpha_2+\mu+\epsilon)Q(t) + \gamma I(t), \\ \lambda^{q-1}\,{}_0^C\mathscr{D}_t^q R(t) = -(\mu+\varphi_1)R(t) + \epsilon Q(t), \\ \lambda^{q-1}\,{}_0^C\mathscr{D}_t^q V(t) = -(\varphi_2+\mu)V(t) + \psi S(t), \\ \lambda^{q-1}\,{}_0^C\mathscr{D}_t^q C(t) = -\sigma C(t) + \theta I(t), \end{cases} \tag{16}$$

accompanying with the initial conditions $S(0) = S_0, I(0) = I_0, Q(0) = Q_0, R(0) = R_0, V(0) = V_0, C(0) = C_0$, where $S_0, I_0, Q_0, R_0, V_0, C_0 \geqslant 0$.

4. Equilibrium points and basic reproduction number

4.1. Disease-free equilibrium point

The disease-free equilibrium (DFE) point is the steady-state solution in the absence of infection or disease. Hence, to obtain such a point for the model (16), following the study [9], we should equate to zero all time fractional derivatives in Eq. (16)

$$\begin{aligned} {}_0^C\mathscr{D}_t^q S(t) = {}_0^C\mathscr{D}_t^q I(t) = {}_0^C\mathscr{D}_t^q Q(t) = {}_0^C\mathscr{D}_t^q R(t) = {}_0^C\mathscr{D}_t^q V(t) \\ = {}_0^C\mathscr{D}_t^q C(t) = 0, \end{aligned} \tag{17}$$

and solve the resultant nonlinear algebraic system such that the infectious states are zero, *i.e.*,

$$I(t) = Q(t) = R(t) = C(t) = 0. \tag{18}$$

This procedure leads to

$$DFE = \left(S^0, I^0, Q^0, R^0, V^0, C^0\right), \tag{19}$$

where $S^0 = \frac{\Lambda(\varphi_2+\mu)}{(\psi+\mu)(\varphi_2+\mu)-\psi\varphi_2}$, $V^0 = \frac{\Lambda\psi}{(\psi+\mu)(\varphi_2+\mu)-\psi\varphi_2}$, $I^0 = Q^0 = R^0 = C^0 = 0$, and $(\psi+\mu)(\varphi_2+\mu) - \psi\varphi_2 > 0$.

4.2. Basic reproduction number

The basic reproduction (BR) number, indicated by R_0, is one of the most important quantities in the epidemiology. The aforementioned quantity denotes the expected number of infectious cases in the population who are susceptible to the infection directly caused by an infectious case. This definition assumes that no other individuals are infected or immunized (naturally or by vaccination). There are various methods for determining the BR number; here the next generation matrix is used [34], where R_0 is the spectral radius of this matrix. First, one defines the transmission and transition function matrices F and W as follows

$$F(t) = \begin{bmatrix} 0 \\ \frac{\beta C(t) S(t)}{C(t)+\rho} \\ 0 \\ 0 \\ 0 \\ 0 \end{bmatrix}, \tag{20}$$

$$W(t) = \begin{bmatrix} (\psi+\mu)S(t) - (\Lambda + \varphi_1 R(t) + \varphi_2 V(t)) + \frac{\beta S(t) C(t)}{C(t)+\rho} \\ (\alpha_1+\mu+\gamma)I(t) \\ (\alpha_2+\mu+\epsilon)Q(t) - \gamma I(t) \\ (\mu+\varphi_1)R(t) - \epsilon Q(t) \\ (\varphi_2+\mu)V(t) - \psi S(t) \\ \sigma C(t) - \theta I(t) \end{bmatrix}. \tag{21}$$

Therefore, we have

$$\begin{bmatrix} \lambda^{q-1}\,{}_0^C\mathscr{D}_t^q S(t) \\ \lambda^{q-1}\,{}_0^C\mathscr{D}_t^q I(t) \\ \lambda^{q-1}\,{}_0^C\mathscr{D}_t^q Q(t) \\ \lambda^{q-1}\,{}_0^C\mathscr{D}_t^q R(t) \\ \lambda^{q-1}\,{}_0^C\mathscr{D}_t^q V(t) \\ \lambda^{q-1}\,{}_0^C\mathscr{D}_t^q C(t) \end{bmatrix} = F(t) - W(t). \tag{22}$$

Evaluating the Jacobian matrices of $F(t)$ and $W(t)$ at the DFE point yields the following matrices

$$F^0 = \begin{bmatrix} 0 & 0 & 0 & 0 & 0 & 0 \\ 0 & 0 & 0 & 0 & 0 & \frac{\beta\Lambda(\varphi_2+\mu)}{((\psi+\mu)(\varphi_2+\mu)-\psi\varphi_2)\rho} \\ 0 & 0 & 0 & 0 & 0 & 0 \\ 0 & 0 & 0 & 0 & 0 & 0 \\ 0 & 0 & 0 & 0 & 0 & 0 \\ 0 & 0 & 0 & 0 & 0 & 0 \end{bmatrix}, \tag{23}$$

$$W^0=\begin{bmatrix}\psi+\mu & 0 & 0 & -\varphi_1 & -\varphi_2 & \frac{\beta\Lambda(\varphi_2+\mu)}{((\psi+\mu)(\varphi_2+\mu)-\psi\varphi_2)\rho}\\ 0 & \alpha_1+\mu+\gamma & 0 & 0 & 0 & 0\\ 0 & -\gamma & \alpha_2+\mu+\epsilon & 0 & 0 & 0\\ 0 & 0 & -\epsilon & \varphi_1+\mu & 0 & 0\\ -\psi & 0 & 0 & 0 & \varphi_2+\mu & 0\\ 0 & -\theta & 0 & 0 & 0 & \sigma\end{bmatrix}. \tag{24}$$

Thus, R_0, the dominant eigenvalue of $F^0\left(W^0\right)^{-1}$, is given by

$$R_0=\frac{\beta\Lambda(\varphi_2+\mu)\theta}{((\psi+\mu)(\varphi_2+\mu)-\psi\varphi_2)(\alpha_1+\mu+\gamma)\rho\sigma}. \tag{25}$$

4.3. Endemic equilibrium point

For obtaining the endemic equilibrium point, we set all fractional derivatives in the system (16) equal to zero, while the number of infectious population is not zero. Let the basic reproduction number $R_0>1$ and $\pi_0=\psi+\mu, \pi_1=\gamma+\ \alpha_1+\mu$, $\pi_2=\epsilon+\alpha_2+\mu, \pi_3=\varphi_1+\mu$, and $\pi_4=\varphi_2+\mu$; then the endemic equilibrium point is

$$E^*=(S^*,I^*,Q^*,R^*,V^*,C^*), \tag{26}$$

where

$$\begin{aligned}
S^*&=\tfrac{\pi_1\pi_2\{\rho\sigma(\pi_1\pi_2\pi_3-\gamma\epsilon\varphi_1)+\Lambda\theta\pi_2\pi_3\}}{\theta\Delta},\\
I^*&=\tfrac{\pi_1\pi_3\{\beta\Lambda\theta\pi_4-(\pi_0\pi_4-\psi\varphi_2)\rho\sigma\pi_1\}}{\theta\Delta},\\
Q^*&=\tfrac{\pi_3\gamma\{\beta\Lambda\theta\pi_4-(\pi_0\pi_4-\psi\varphi_2)\rho\sigma\pi_1\}}{\theta\Delta},\\
R^*&=\tfrac{\gamma\epsilon\{\beta\Lambda\theta\pi_4-(\pi_0\pi_4-\psi\varphi_2)\rho\sigma\pi_1\}}{\theta\Delta},\\
V^*&=\tfrac{\pi_1\psi\{\rho\sigma(\pi_1\pi_2\pi_3-\gamma\epsilon\varphi_1)+\Lambda\theta\pi_2\pi_3\}}{\theta\Delta},\\
C^*&=\tfrac{\pi_2\pi_3\{\beta\Lambda\theta\pi_4-(\pi_0\pi_4-\psi\varphi_2)\rho\sigma\pi_1\}}{\sigma\Delta},
\end{aligned} \tag{27}$$

and $\Delta=\pi_1\pi_2\pi_3(\pi_0\pi_4-\psi\varphi_2)+\beta\pi_4(\pi_1\pi_2\pi_3-\gamma\epsilon\varphi_1)$. As can be seen, the symbol Δ in the denominators depends on the system's parameters. Thus, the values of parameters in the model (16) should be selected in such a way that $\Delta\neq 0$.

5. Numerical method

In this section, the product-integration rule is used to obtain a numerical scheme solving the model (16). To this end, consider the following fractional initial-value problem

$$\lambda^{q-1}\,{}_0^C\mathscr{D}_t^q y(t)=f(t,y(t)), \tag{28}$$

with the initial condition $y(t_0)=y_0$. By applying the operator ${}_0\mathscr{I}_t^q$ on the both sides of (28), we have the next integral equation

$$y(t)=y_0+\lambda^{1-q}\int_0^t f(x,y(x))m_L(t-x)dx. \tag{29}$$

Let h be the time step size, and put $t=t_n=nh$ in the Eq. (29), so we achieve

$$y(t_n)=y_0+\lambda^{1-q}\sum_{i=0}^{n-1}\int_{t_i}^{t_{i+1}} f(x,y(x))m_L(t_n-x)dx. \tag{30}$$

Then the first-order Lagrange interpolation is used to approximate $f(t,y(t))$ in $[t_i,t_{i+1}]$. Thus, the following general form of product-integration formula is attained

$$\begin{aligned}
y_n&=y_0+\\
&\lambda^{1-q}\sum_{i=0}^{n-1}\left(\tfrac{(h+1)f\left(t_{i+1},y_{i+1}\right)-f(t_i,y_i)}{h}\right)\int_{t_i}^{t_{i+1}}(x-t_{i+1})m_L(t_n-x)dx, n\geqslant 1,
\end{aligned} \tag{31}$$

where $y_i=y(t_i)$. Note that the Eq. (31) is an implicit equation for y_n, so one can use the Newton-Raphson iterative method to evaluate the successive approximations. Moreover, the order of convergence for the above rule is $1+q$ for $0<q<1$(see [35]). Additionally, here we consider three special cases for the method (31):

- If $\kappa_L(t)=\frac{t^{-q}}{\Gamma(1-q)}$, then the following formula is obtained

$$y_n=y_0+\lambda^{1-q}h^q\left(\widehat{\omega}_n f(t_0,y_0)+\sum_{i=1}^{n}\omega_{n-i}f(t_i,y_i)\right), \tag{32}$$

where

$$\widehat{\omega}_n=\frac{(n-1)^{q+1}-n^q(n-q-1)}{\Gamma(q+2)}, \tag{33}$$

$$\omega_i=\begin{cases}\frac{1}{\Gamma(2+q)}, & i=0,\\ \frac{(n-1)^{1+q}-2n^{1+q}+(n+1)^{1+q}}{\Gamma(2+q)}, & i=1,2,\cdots,n-1.\end{cases} \tag{34}$$

- If $\kappa_L(t)=\frac{\chi(q)}{1-q}E_q\left[\frac{-q}{1-q}t^q\right]$, then

$$y_n=y_0+\lambda^{1-q}\frac{h^q}{\chi(q)}\left(\widehat{\omega}_n f(t_0,y_0)+\sum_{i=1}^{n}\omega_{n-i}f(t_i,y_i)\right), \tag{35}$$

where

$$\widehat{\omega}_n=\frac{(n-1)^{q+1}-n^q(n-q-1)}{\Gamma(q+2)}, \tag{36}$$

$$\omega_i=\begin{cases}\frac{1}{\Gamma(2+q)}+\frac{1-q}{qh^q}, & i=0,\\ \frac{(n-1)^{1+q}-2n^{1+q}+(n+1)^{1+q}}{\Gamma(2+q)}, & i=1,2,\cdots,n-1.\end{cases} \tag{37}$$

- If $\kappa_L(t)=\frac{\chi(q)}{1-q}\exp\left[\frac{-q}{1-q}t\right]$, then

$$y_n=y_0+\frac{\lambda^{1-q}h}{\chi(q)(2-q)}\left(qf(t_0,y_0)+\sum_{i=1}^{n}\omega_{n-i}f(t_i,y_i)\right), \tag{38}$$

where

$$\omega_i=\begin{cases}\frac{2(1-q)}{h}+q, & i=0,\\ 2q, & i=1,2,\cdots,n-1.\end{cases} \tag{39}$$

5.1. Simulation results and discussion

In this section, we discuss the cholera outbreak happened in Yemen from April 27, 2017, to April 15, 2018 [4]. To do so, we apply the numerical algorithm expressed above to solve the integer and fractional-order systems (15) and (16), respectively. In these simulations, the values of biological parameters are selected according to [9], which are also given in Table 1.

Table 1 Values of parameters [9].

Parameter	Λ	μ	β	ρ	φ_1	φ_2
Value	$\frac{28.4N(0)}{365000}$	1.6×10^{-5}	0.01694	10^7	$\frac{0.4}{365}$	$\frac{1}{1460}$
Parameter	ψ	γ	α_1	α_2	θ	σ
Value	0.005	1.15	6×10^{-6}	3×10^6	10	0.33
Parameter	$S(0)$	$I(0)$	$Q(0)$	$R(0)$	$V(0)$	$B(0)$
Value	28249670	750	0	0	0	275000

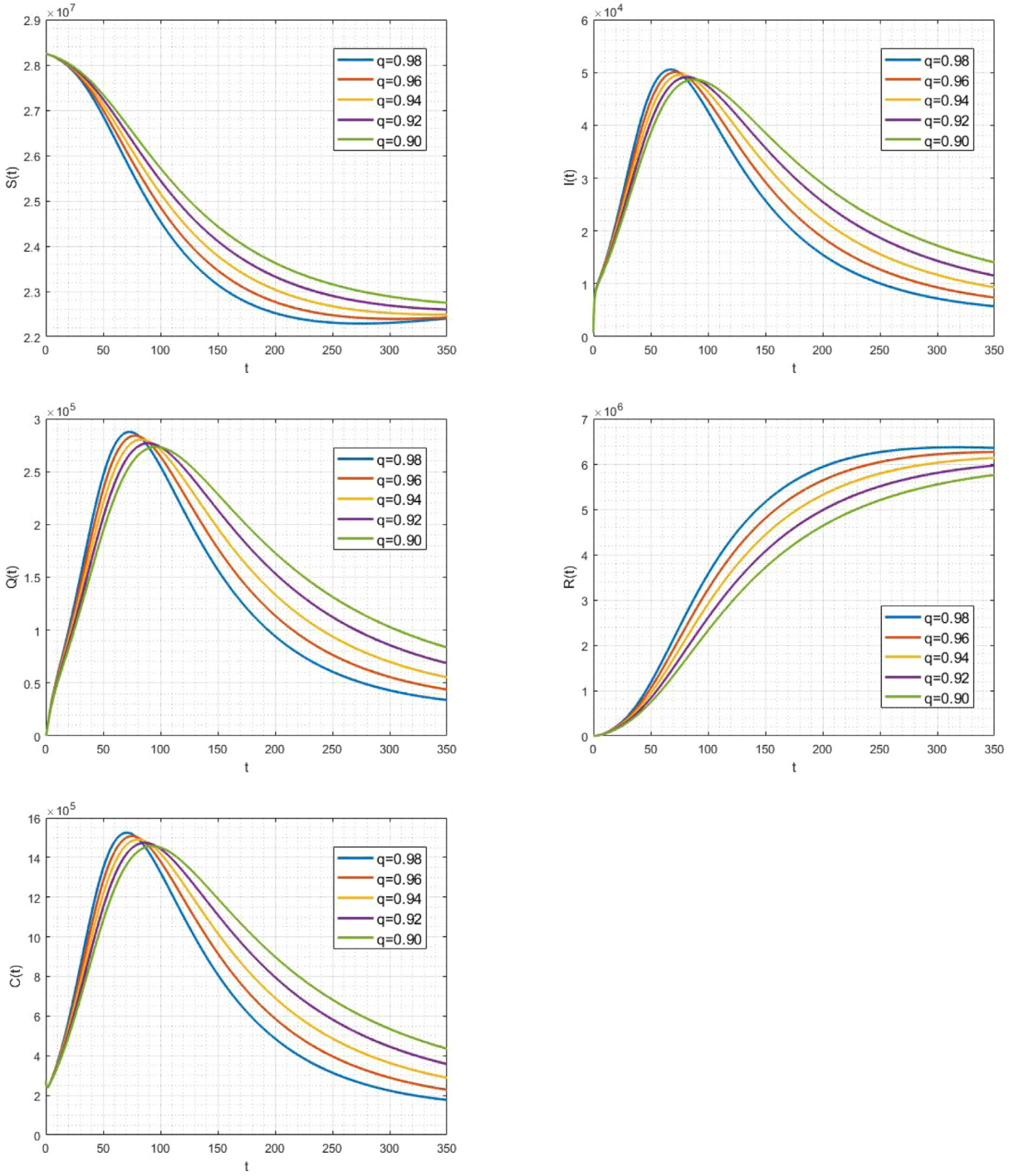

Fig. 1 Simulation results for the model (16) without vaccination when $\kappa_L(t) = \frac{t^{-q}}{\Gamma(1-q)}$.

The dynamical behaviours of the new model (16) without vaccination intervention for different kernels and various fractional orders are illustrated in Figs. 1–3. In these figures, the numerical simulations are performed with the mentioned values in Table 1 for the parameters except $\varphi_2 = \psi = 0$. Figs. 1–3 indicate that the susceptible population $S(t)$ grows uniformly whenever the non-integer order q decreases. Also, there is a sharp leap in the population of infectious people in the early years when q decreases. Furthermore, as can be seen from Figs. 1,2, when the power and ML kernels are used, the recovered population $R(t)$ decreases by decreasing q. Besides, Fig. 3 depicts that there is a decline in the recovered population in the early years by decreasing the fractional order q when the exponential kernel is applied. In Fig. 4, different kernels in the general form of Caputo fractional derivative are considered. Moreover, a systematic comparison is performed between our results and those of the classic integer model (15) and real data. Fig. 4(a) indicates that the fractional-order $q = 0.96$ is

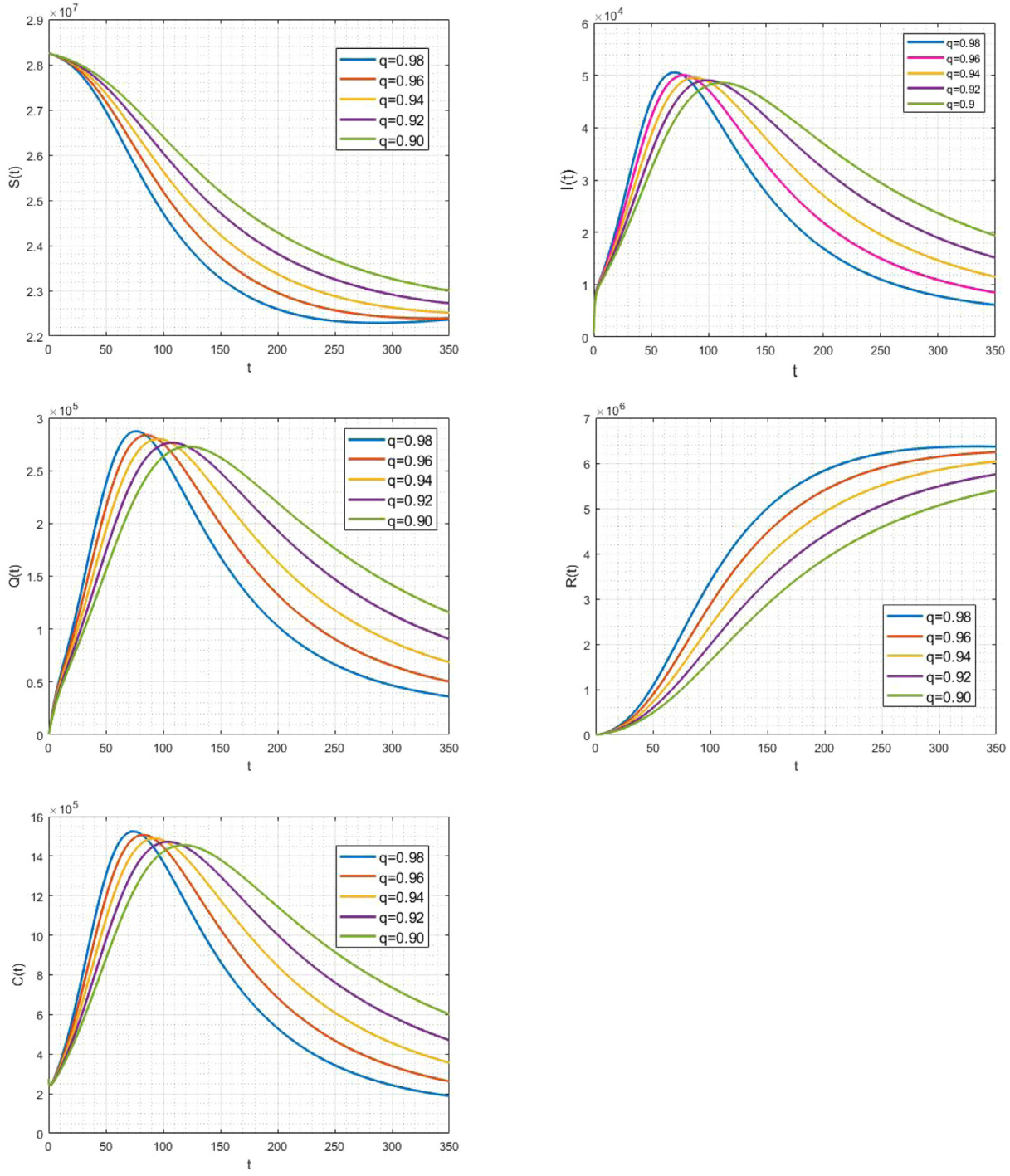

Fig. 2 Simulation results for the model (16) without vaccination when $\kappa_L(t) = \frac{\chi(q)}{1-q} E_q\left[\frac{-q}{1-q} t^q\right]$.

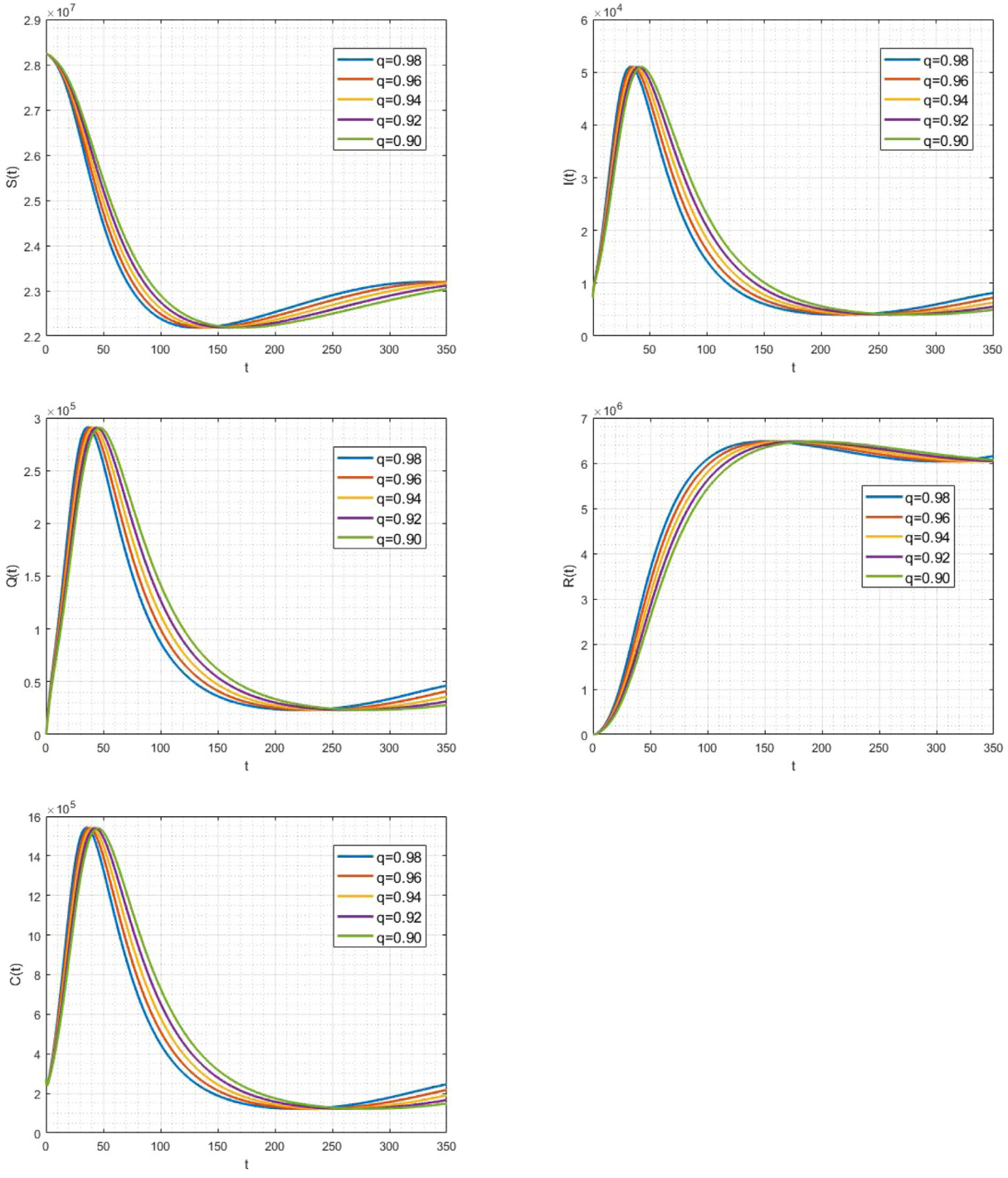

Fig. 3 Simulation results for the model (16) without vaccination when $\kappa_L(t) = \frac{\chi(q)}{1-q} \exp\left[\frac{-q}{1-q}t\right]$.

more consistent with the real data when the power kernel is applied. Also, from Figs. 4(b) and 4(c) it is apparent that the fractional orders $q = 0.98$ and $q = 0.90$ are more consistent with the real data when the kernels are the ML and exponential functions, respectively. Simulations of the infected individuals for each kernel with its best fractional order are compared in Fig. 4(d). This figure reveals that the numerical results when the kernel is the ML function are closer to the real data. Thus, the model (16) with the ML kernel and non-integer order $q = 0.98$ as the best candidate is applied to describe the effect of vaccination on the considered cholera outbreak in Yemen. In this case, the dynamical behaviour of the new fractional model under the effect of vaccination treatment is depicted in Fig. 5. The predicted number of infected individuals under vaccination campaign (Fig. 5) reveals that the spread of cholera would have considerably been decreased, so there would not have been so many deaths if the vaccination had been done earlier in time.

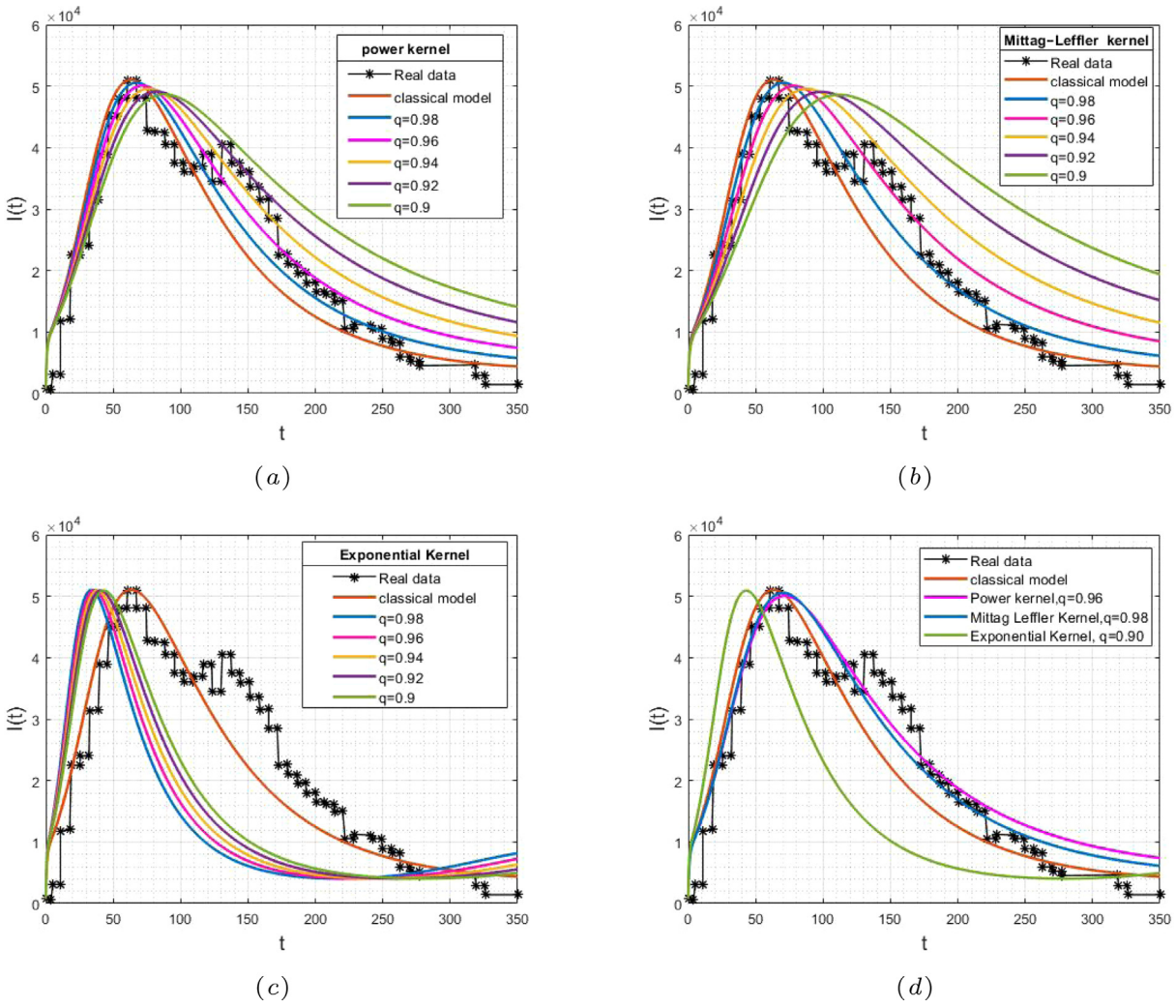

Fig. 4 The evolution of infectious individuals for different kernels and various fractional orders.

Remark 5.1. As mentioned before, comparative and simulation results in this study are related to the cholera outbreak in Yemen from April 27, 2017, to April 15, 2018, and according to the real data supported by WHO [5]. To extend these results for any other cases, we need a new set of real data related to each new case; then, by using this new information, we have to update the values of parameters and coefficients, evaluate different kernel functions, and try various fractional orders in order to find the best model describing the new case under consideration. Here, it should be noted that the output of this research provides such a degree-of-freedom for the modelling of a new epidemic outbreak; indeed, for each new case, the general fractional model has to be updated in terms of its parameters, coefficients, the kernel of fractional derivative, and its associated fractional order, in order to build up the best model following the new set of real data better than the other classical and fractional frameworks.

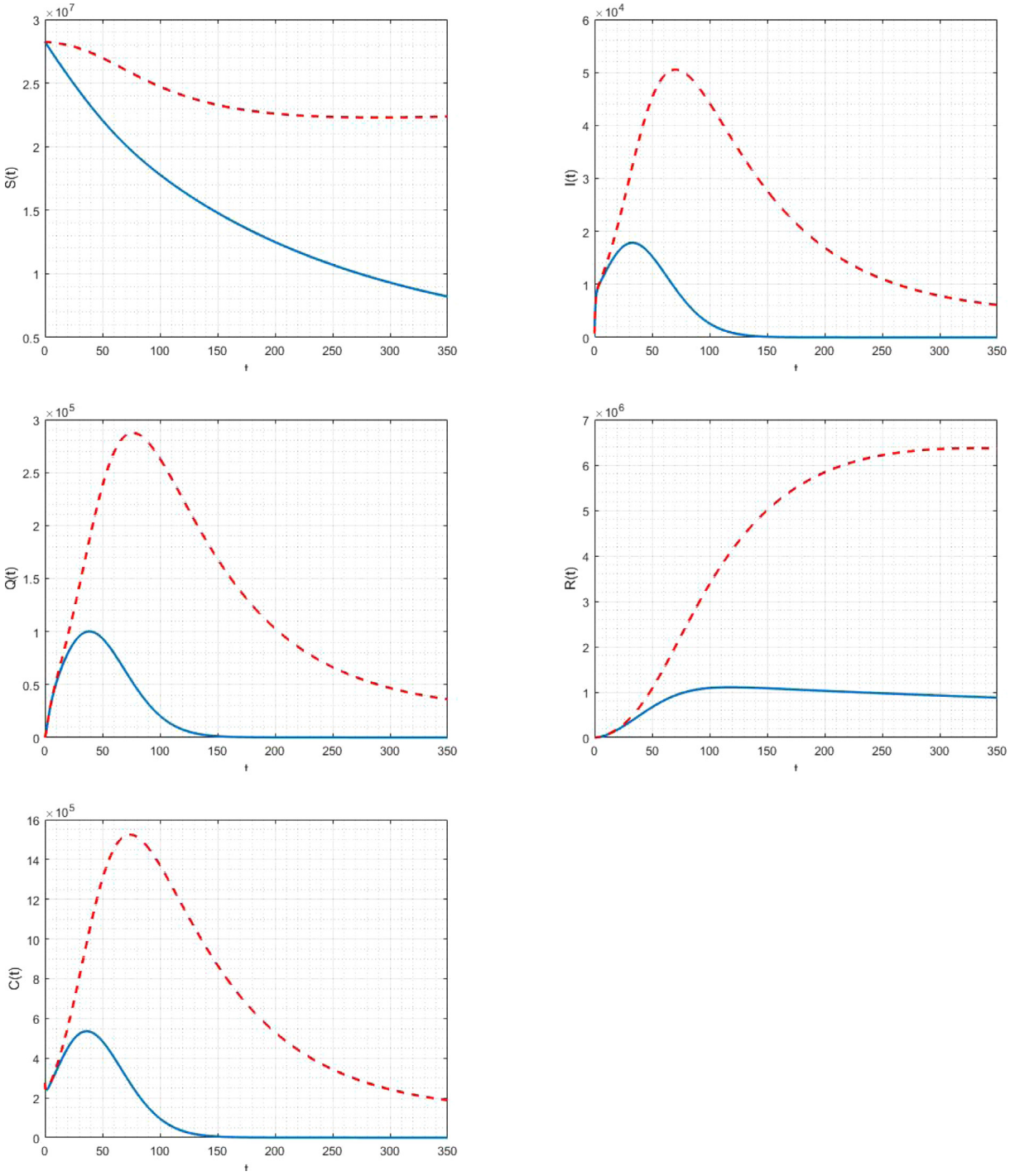

Fig. 5 The plots of the new model (16) without vaccination (red dashed line) and with vaccination (blue solid line) when $\kappa_L(t) = \frac{\chi(q)}{1-q} E_q\left[\frac{-q}{1-q} t^q\right]$ and $q = 0.98$.

6. Conclusion

In this paper, we developed a new mathematical model involving the general form of Caputo fractional derivative for a real cholera outbreak in Yemen. The steady-states and the basic reproduction number were computed analytically. Besides, a new scheme was designed to implement the model numerically. To observe the efficiency of using a general kernel in the new modelling strategy, several numerical simulations were performed in Figs. 1–3 for different kernels and various fractional orders. These simulations disclosed that changes in the kernel and fractional order influence the model's dynamical behaviours effectively. Additionally, we found an appropriate kernel function and a suitable fractional order in Fig. 4 by some comparative results with a set of real clinical observations. Fig. 4 revealed that the numerical results with the ML kernel and $q = 0.98$ are closer to the real data than the other classical and fractional frameworks. Thus, the fractional model with the ML kernel and the non-integer order $q = 0.98$ was selected to

describe the effect of vaccination on the cholera disease under investigation. In this case, the dynamical behaviours of the new fractional model under the treatment of vaccination were depicted in Fig. 5. Simulation results in this figure portrayed that the number of infected individuals, associated with the cholera outbreak in Yemen from April 27, 2017, to April 15, 2018, would have considerably been decreased under vaccination campaign, so there would not have been so many deaths, if the vaccination had been done earlier in time. However, as the vaccination was not started early in time for the aforesaid outbreak, so many deaths occurred. Therefore, the prediction in our study, indeed, presens a regret for a past event.

Nowadays, cholera infection is still a health-care problem in many parts of the world and causes widespread human suffering; therefore, the dynamical investigation and control of this infectious disease should be the goal of many researches these days. As a result, further studies should be done on the stability analysis [36] and the implementation of other control methodologies, such as optimal control [37], in the presence of epidemic infectious diseases such as cholera, Ebola, COVID-19, etc.

Declaration of Competing Interest

The authors declare that they have no known competing financial interests or personal relationships that could have appeared to influence the work reported in this paper.

Acknowledgements

The research of JJN has been partially supported by Xunta de Galicia, grant ED431C 2019/02 for Competitive Reference Research Groups (2019–22), and by Instituto de Salud Carlos III, grant COV20/00617.

References

[1] A.P. Lemos-Paião, C.J. Silva, D.F.M. Torres, An epidemic model for cholera with optimal control treatment, J. Comput. Appl. Math. 318 (2017) 168–180.
[2] R. Ratnayake, F. Finger, A.S. Azman, D. Lantagne, S. Funk, W.J. Edmunds, F. Checchi, Highly targeted spatiotemporal interventions against cholera epidemics, 2000–19: a scoping review, Lancet. Infect. Dis. 21 (3) (2021) e37–e48.
[3] M. Ali, A.R. Nelson, A.L. Lopez, D.A. Sack, Updated global burden of cholera in endemic countries, PLOS Neglected Trop. Dis. 9 (6) (2015) e0003832.
[4] World Health Organization, Yemen: Weekly Cholera Bulletins, 21st May 2018.
[5] The Telegraph News: Race against time to curb cholera outbreak in Yemen, 09th May 2018. Available from: https://www.telegraph.co.uk/news/0/race-against-time-curb-cholera-outbreak-yemen/.
[6] D. Baleanu, M. Hassan Abadi, A. Jajarmi, K. Zarghami Vahid, J.J. Nieto, A new comparative study on the general fractional model of COVID-19 with isolation and quarantine effects, Alexandr. Eng. J. 61 (6) (2022) 4779–4791.
[7] A. Jajarmi, D. Baleanu, K. Zarghami Vahid, S. Mobayen, A general fractional formulation and tracking control for immunogenic tumor dynamics, Math. Methods Appl. Sci. 45 (2) (2022) 667–680.
[8] Y. Wang, T. Abdeljawad, A. Din, Modeling the dynamics of stochastic norovirus epidemic model with time-delay, Fractals (2022). https://doi.org/10.1142/S0218348X22401508.
[9] A.P. Lemos-Paião, C.J. Silva, D.F.M. Torres, A cholera mathematical model with vaccination and the biggest outbreak of world's history, AIMS Math. 3 (4) (2018) 448–463.
[10] V. Capasso, S.L. Paveri-Fontana, A mathematical model for the 1973 cholera epidemic in the European Mediterranean region, Revue d'Epidémiologie et de Santé Publique 27 (2) (1979) 121–132.
[11] H. Nishiura, S. Tsuzuki, B. Yuan, T. Yamaguchi, Y. Asai, Transmission dynamics of cholera in Yemen, 2017: a real time forecasting, Theoret. Biol. Med. Model. 14 (2017) 14.
[12] R.L.M. Neilan, E. Schaefer, H. Gaff, K.R. Fister, S. Lenhart, Modeling optimal intervention strategies for cholera, Bull. Math. Biol. 72 (2010) 2004–2018.
[13] A.P. Lemos-Paião, C.J. Silva, D.F.M. Torres, E. Venturino, Optimal control of aquatic diseases: a case study of Yemen's cholera outbreak, J. Optim. Theory Appl. 185 (2020) 1008–1030.
[14] D. Baleanu, S.S. Sajjadi, J.H. Asad, A. Jajarmi, E. Estiri, Hyperchaotic behaviours, optimal control, and synchronization of a nonautonomous cardiac conduction system, Adv. Difference Eqs. 2021 (2021) 157.
[15] D. Baleanu, S.S. Sajjadi, A. Jajarmi, Ö. Defterli, On a nonlinear dynamical system with both chaotic and non-chaotic behaviours: a new fractional analysis and control, Adv. Difference Eqs. 2021 (2021) 234.
[16] V.S. Erturk, E. Godwe, D. Baleanu, P. Kumar, J.H. Asad, A. Jajarmi, Novel fractional-order Lagrangian to describe motion of beam on nanowire, Acta Phys. Pol., A 140 (3) (2021) 265–272.
[17] M.S. Abdo, S.K. Panchal, K. Shah, T. Abdeljawad, Existence theory and numerical analysis of three species prey-predator model under Mittag-Leffler power law, Adv. Difference Eqs. 2020 (2020) 249.
[18] W. Shatanawi, M.S. Abdo, M.A. Abdulwasaa, K. Shah, S.K. Panchal, S.V. Kawale, K.P. Ghadle, A fractional dynamics of tuberculosis (TB) model in the frame of generalized Atangana-Baleanu derivative, Res. Phys. 29 (2021) 104739.
[19] D. Ziane, M.H. Cherif, C. Cattani, K. Belghaba, Yang-Laplace decomposition method for nonlinear system of local fractional partial differential equations, Appl. Math. Nonlinear Sci. 4 (2) (2019) 489–502.
[20] E. Ilhan, I.O. Kiymaz, A generalization of truncated M-fractional derivative and applications to fractional differential equations, Appl. Math. Nonlinear Sci. 5 (1) (2020) 171–188.
[21] D. Kaur, P. Agarwal, M. Rakshit, M. Chand, Fractional calculus involving (p, q)-Mathieu type series, Appl. Math. Nonlinear Sci. 5 (2) (2020) 15–34.
[22] F. Evirgen, S. Uçar, N. Özdemir, System analysis of HIV infection model with $CD4^+T$ under non-singular kernel derivative, Appl. Math. Nonlinear Sci. 5 (1) (2020) 139–146.
[23] F. Bozkurt, A. Yousef, T. Abdeljawad, A. Kalinli, Q. Al Mdallal, A fractional-order model of COVID-19 considering the fear effect of the media and social networks on the community, Chaos Solitons Fract. 152 (2021) 111403.
[24] S.S. Redhwan, M.S. Abdo, K. Shah, T. Abdeljawad, S. Dawood, H.A. Abdo, S.L. Shaikh, Mathematical modeling for the outbreak of the coronavirus (COVID-19) under fractional nonlocal operator, Res. Phys. 19 (2020) 103610.
[25] M. Farman, A. Akgül, T. Abdeljawad, P.A. Naik, N. Bukhari, A. Ahmad, Modeling and analysis of fractional order Ebola virus model with Mittag-Leffler kernel, Alexandr. Eng. J. 61 (3) (2022) 2062–2073.
[26] D. Baleanu, S. Zibaei, M. Namjoo, A. Jajarmi, A nonstandard finite difference scheme for the modelling and nonidentical synchronization of a novel fractional chaotic system, Adv. Difference Eqs. 2021 (2021) 308.
[27] Y. Luchko, M. Yamamoto, General time-fractional diffusion equation: some uniqueness and existence results for the initial-boundary-value problems, Fract. Calculus Appl. Anal. 19 (3) (2016) 676–695.

[28] A. Jajarmi, D. Baleanu, K. Zarghami Vahid, H. Mohammadi Pirouz, J.H. Asad, A new and general fractional Lagrangian approach: a capacitor microphone case study, Res. Phys. 31 (2021) 104950.
[29] O.P. Agrawal, Generalized variational problems and Euler-Lagrange equations, Comput. Math. Appl. 59 (2010) 1852–1864.
[30] I. Podlubny, Fractional Differential Equations: An Introduction to Fractional Derivatives, Fractional Differential Equations, to Methods of Their Solution and Some of Their Applications, Academic Press, New York, 1999.
[31] A. Atangana, D. Baleanu, New fractional derivatives with nonlocal and non-singular kernel: theory and application to heat transfer model, Therm. Sci. 20 (2) (2016) 763–769.
[32] M. Caputo, M. Fabrizio, A new definition of fractional derivative without singular kernel, Prog. Fract. Different. Appl. 1 (2015) 73–75.
[33] J.F. Gómez-Aguilar, J.J. Rosales-García, J.J. Bernal-Alvarado, T. Córdova-Fraga, R. Guzmán-Cabrera, Fractional mechanical oscillators, Revista Mexicana de Física 58 (2012) 348–352.
[34] J.M. Heffernan, R.J. Smith, L.M. Wahl, Perspectives on the basic reproductive ratio, J. Roy. Soc. Interface 2 (2005) 281–293.
[35] R. Garrappa, Numerical solution of fractional differential equations: a survey and a software tutorial, Mathematics 6 (2) (2018) 16.
[36] A.A. Abozaid, H.H. Selim, K.A.K. Gadallah, I.A. Hassan, E.I. Abouelmagd, Periodic orbit in the frame work of restricted three bodies under the asteroids belt effect, Appl. Math. Nonlinear Sci. 5 (2) (2020) 157–176.
[37] A. Jajarmi, N. Pariz, S. Effati, A.V. Kamyad, Infinite horizon optimal control for nonlinear interconnected large-scale dynamical systems with an application to optimal attitude control, Asian J. Control 14 (5) (2012) 1239–1250.